British Journal of Cancer (2011), 1 – 7

www.bjcancer.com

Full Paper

Cancer cell proliferation is inhibited by specific modulation frequencies

JW Zimmerman[1], MJ Pennison[1], I Brezovich[2], N Yi[3], CT Yang[3], R Ramaker[1], D Absher[4], RM Myers[4], N Kuster[5], FP Costa[6], A Barbault[7] and B Pasche[*,1]

[1]Division of Hematology/Oncology, Department of Medicine, University of Alabama at Birmingham and UAB Comprehensive Cancer Center, 1802 6th Avenue South, NP 2566, Birmingham, AL 35294-3300, USA; [2]Department of Radiation Oncology, University of Alabama at Birmingham and UAB Comprehensive Cancer Center, Birmingham, AL 35294, USA; [3]Section of Statistical Genetics, Department of Biostatistics, School of Public Health, The University of Alabama at Birmingham, Birmingham, AL 35294, USA; [4]HudsonAlpha Institute for Biotechnology, Huntsville, AL 35806, USA; [5]IT'IS Foundation, Swiss Federal Institute of Technology, Zurich, Switzerland; [6]Department of Transplantation and Liver Surgery, Hospital das Clínicas, University of São Paulo, São Paulo, Brazil; [7]Rue de Verdun 20, Colmar 68000, France

BACKGROUND: There is clinical evidence that very low and safe levels of amplitude-modulated electromagnetic fields administered via an intrabuccal spoon-shaped probe may elicit therapeutic responses in patients with cancer. However, there is no known mechanism explaining the anti-proliferative effect of very low intensity electromagnetic fields.

METHODS: To understand the mechanism of this novel approach, hepatocellular carcinoma (HCC) cells were exposed to 27.12 MHz radiofrequency electromagnetic fields using *in vitro* exposure systems designed to replicate *in vivo* conditions. Cancer cells were exposed to tumour-specific modulation frequencies, previously identified by biofeedback methods in patients with a diagnosis of cancer. Control modulation frequencies consisted of randomly chosen modulation frequencies within the same 100 Hz–21 kHz range as cancer-specific frequencies.

RESULTS: The growth of HCC and breast cancer cells was significantly decreased by HCC-specific and breast cancer-specific modulation frequencies, respectively. However, the same frequencies did not affect proliferation of nonmalignant hepatocytes or breast epithelial cells. Inhibition of HCC cell proliferation was associated with downregulation of *XCL2* and *PLP2*. Furthermore, HCC-specific modulation frequencies disrupted the mitotic spindle.

CONCLUSION: These findings uncover a novel mechanism controlling the growth of cancer cells at specific modulation frequencies without affecting normal tissues, which may have broad implications in oncology.

British Journal of Cancer advance online publication, 1 December 2011; doi:10.1038/bjc.2011.523 www.bjcancer.com

Keywords: hepatocelullar carcinoma; electromagnetic fields; mitotic spindle; PLP2; XCL2

Treatment of hepatocellular carcinoma (HCC) is a major challenge given the limited number of therapeutic options available (Thomas and Zhu, 2005). We have developed a novel approach to treat advanced HCC, consisting of intrabuccal administration of very low levels of radiofrequency electromagnetic fields (RF EMF), amplitude-modulated at specific frequencies, and identified using biofeedback methods in patients with cancer (Barbault *et al*, 2009). The encouraging findings from a feasibility study (Barbault *et al*, 2009) led to the design of a phase I/II trial in patients with advanced HCC, and objective responses assessed by CT-scan and changes in alpha-fetoprotein levels were observed in several patients with biopsy-proven HCC (Costa *et al*, 2011). These findings prompted us to initiate reverse translational experiments to investigate the mechanism of action of amplitude-modulated electromagnetic fields. Two different *in vitro* exposure systems operating at 27.12 MHz were used to expose cells in culture, replicating patient-treatment conditions.

Proliferation of both HepG2 and Huh7 HCC cells was significantly decreased upon exposure to radiofrequency electromagnetic fields, which were modulated at HCC-specific modulation frequencies. To determine how such frequencies modulate cancer cell growth, we assessed differential gene expression with RNA-seq and found that the expression of several genes was significantly downregulated by HCC-specific modulation frequencies. Previous reports have shown that low intensity, intermediate frequency electric fields are capable of inhibiting cancer growth by interfering with the proper formation of the mitotic spindle (Kirson *et al*, 2004; Kirson *et al*, 2007). Similarly, we found that electromagnetic fields that are amplitude-modulated at HCC-specific frequencies disrupt the mitotic spindle of HCC cells. Thus, we provide novel evidence that very low level of amplitude-modulated electromagnetic fields block the growth of HCC cells in a tumour- and tissue-specific fashion.

*Correspondence: Dr B Pasche; E-mail: Boris.Pasche@ccc.uab.edu
Received 10 October 2011; accepted 7 November 2011

MATERIALS AND METHODS

In vitro exposure devices

The design and construction of the two *in vivo* exposure devices (Figure 1) used to conduct these experiments is described in the Supplementary Information.

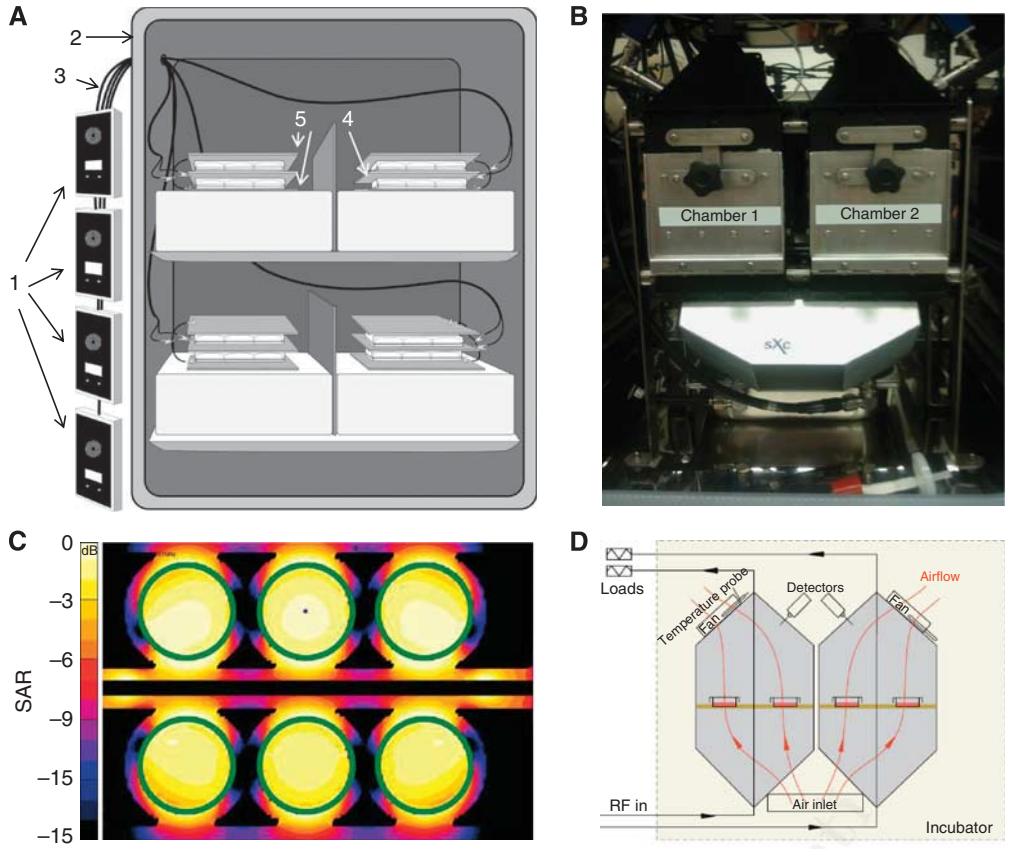

Figure 1 *In vitro* exposure experimental setups. (**A**) Parallel plate capacitor. Emitting devices (1) are placed outside the incubator (2). Each device is connected to a coaxial cable (3), which is connected to a set of brass plates inside the incubator. The centre brass plate (4) is connected to the inner conductor of the emitting device coaxial cable. The outer two brass plates (5) are connected to the outer conductor of the emitting device coaxial cable. Plates containing cells are placed in between the brass plates. (**B**) TEM cell. The system contains two identical TEM cells placed in an incubator. (**C**) Distribution of the specific absorption rate (SAR) of cell monolayer in the TEM cell (1 dB per contour), (**D**) Schematic representation showing the air flow through the TEM cell.

Cell lines

HepG2 and Huh7 cells, both of Biosafety Level 1, were used as representative HCC cell lines. HepG2 cells were obtained from ATCC (Manassas, VA, USA), and Huh7 cells were a gift from Dr Nareej Saxena (Emory University). Normal hepatocytes, THLE-2 cells, were also obtained from ATCC. The breast adenocarcinoma cell line MCF-7 was used as a representative non-HCC malignant cell line (ATCC). The breast epithelial cell line MCF-10A (ATCC) was used to represent normal breast cells. Lymphoblastoid cell lines from healthy individuals enrolled in IRB-approved protocols were provided by Dr Jeff Edberg (UAB).

[^{3}H]thymidine incorporation assay

Growth inhibition (GI) was assessed in HCC cells exposed to HCC-specific modulation frequencies as previously described (Rosman *et al*, 2008).

Luminescent cell viability assay

Cell proliferation was quantitated using the Promega CellTiter-Glo Luminescent Cell Viability Assay (Promega, Madison, WI, USA), a method to determine the number of viable cells in culture based on ATP quantitation.

RNA-seq

We performed RNA-seq as previously described (Reddy *et al*, 2009). We used HepG2 cells exposed to either HCC-specific modulation frequencies or to randomly chosen frequencies. We double-selected polyA-containing mRNA from 3 μg of total RNA by using oligo-dT magnetic beads. We fragmented the mRNA with RNA fragmentation buffer and removed free-ions with a G-50 Sepharose spin column. Fragmented mRNA was used as a template to synthesise single-stranded cDNA with SuperScript II reverse transcriptase with random hexamer primers in the presence of RNAseOUT (Invitrogen by Life Technologies Corporation, Carlsbad, CA, USA). We synthesised double-stranded DNA (dsDNA) for sequencing by ligating Illumina (Illumina, San Diego, CA, USA) sequencing adaptors to blunted and dA-extended dsDNA, and size-selected fragments of 200–300 bp from a 2% Invitrogen gel and purified with a Qiagen Gel Extraction kit (Qiagen, Valencia, CA, USA). Lastly, we amplified the dsDNA library with 15 rounds of PCR with Illumina sequencing primers. Sequencing was performed on an Illumina GenomeAnalyzer IIx and the paired 36 bp reads were mapped to the hg18 reference genome by using ELAND (Illumina), allowing up to two mismatches per read and 10 or fewer map locations. By using the ERANGE software package (http://woldlab.caltech.edu/rnaseq), we placed uniquely mapped reads against 29 673 transcripts from NCBI build 36.1 of the human genome. After placing unique reads, ERANGE assigned multiple mapping reads and reads mapping to

splice junctions according to the number of unique reads in potential transcripts. Once all reads were mapped, ERANGE reported gene expression in units of reads per kilobase of exon and per million tags sequenced (RPKM).

Quantitative PCR

At the conclusion of the AM-EMF exposure portion of the experiment, RNA extraction (Qiagen) and reverse transcription (TaqMan, Applied Biosystems by Life Technologies Corporation) were performed to generate cDNA. Experiments comparing gene expression in HCC cells receiving HCC-specific AM-EMF with gene expression in HCC cells not receiving any exposure were conducted using Applied Biosystems pre-designed TaqMan Gene Expression Assays (*PLP2,* cat#Hs01099969_g1; *XCL2,* cat#Hs00237019_m1; Applied Biosystems by Life Technologies Corporation). Real-time quantitation was completed in quadruplicate according to the manufacturer's instructions using an ABI 7900HT Real-Time PCR System (ABI by Life Technologies Corporation), with analysis performed using ABI SDS2.2 software. Quantitative values of gene expression were determined by comparing PCR amplification curves to a known standard curve generated in tandem with the experimental samples. Each sample was individually normalised to the average corresponding to endogenous expression of *GAPDH* (*GAPDH*, cat#Hs99999905_m1, TaqMan, Applied Biosystems by Life Technologies Corporation). Averages of the normalised values from each condition were then used to compare the relative gene expression between the experimental groups. The s.e.m. was determined for each experimental condition.

Confocal laser scanning microscopy

Cells undergoing mitosis were imaged using the Zeiss LSM 710 Confocal Laser Scanning Microscope (Carl Zeiss, Inc., Thornwood, NY, USA). For imaging experiments, 22 mm square microscope cover glass (Corning Life Sciences, Lowell, MA, USA, cat#2865 – 22) were flame-sterilised with 200-proof ethanol and placed in 6-well or 35 mm Falcon tissue culture plates (BD Biosciences, Franklin Lakes, NJ, USA). Approximately 300 μl of cell suspension/growth media was added directly to the top of the cover slips, and cells were plated at varying concentrations ($4 \times 10^5 - 5 \times 10^5$ cells per ml) on separate cover slips for each assay to control for variability in antibody affinity between different experiments. Once the cells were given 8 – 18 h to attach to the cover slips, 3 ml of complete growth media was added to each well containing a cover slip. Following RF EMF exposure, indirect immunofluorescent microscopy compared the cells receiving HCC-specific modulation frequencies with cells not receiving any exposure (Microtubule Marker (AE-8) sc-73551, Fluorescent Secondary Alexa Fluor 488 goat anti-mouse IgG (H + L): A-11001; Santa Cruz Biotechnologies, Santa Cruz, CA, USA).

Karyotype analysis

To determine whether these changes were associated with karyotypic changes, HepG2 cells exposed to HCC-specific modulation frequencies or unexposed were harvested, slides prepared, and metaphase chromosomes G-banded using standard methods. The chromosomes were analysed and the karyotype described according to the International System for Cytogenetic Nomenclature (Brothman *et al*, 2009).

Statistical analyses

One sample two-sided *t*-test was performed to test the significance of cell proliferation exposed to RF EMF amplitude-modulated at tumour-specific or randomly chosen frequencies. ANCOVA analysis: For the long-term (7 weeks) GI analysis and the GI analysis for varying SAR values (0.05, 0.1, 0.4, and 1.0 W kg^{-1}), data were fit to a linear model, and time point and dosage level were considered as covariates in determining significance.

RESULTS

Assessment of cell proliferation in the presence of RF EMF

Cell proliferation assays were conducted after 7 days, that is, 21 h of exposure to amplitude-modulated RF EMF. Treatment with HCC-specific modulation frequencies (Supplementary Table 1) significantly reduced the proliferation of HepG2 and Huh7 cells using both the parallel plate capacitor and the transverse electromagnetic (TEM) setups (Figure 1). The observed growth-inhibitory effect on HepG2 cells was of the same magnitude when using a tritium incorporation assay and a bioluminescence assay based on ATP consumption (Figure 2A). Having shown similar results with two different assays, the remainder of the cell proliferation experiments were conducted with the more commonly used tritium incorporation assay. Cell proliferation of HepG2 and Huh7 cells exposed to HCC-specific modulation frequencies was significantly lower than the proliferation of cells exposed either to randomly chosen frequencies (Supplementary Table 2) or not exposed to RF EMF (Figure 2A, columns 1 – 3). When HepG2 cells were exposed for only 1 h daily, we did not observe any significant inhibition of cell proliferation (Figure 2B). Daily exposure for 6 h instead of 3 h resulted in the same level of cell-proliferation inhibition (Figure 2B). To determine when HCC-specific modulation frequencies begin to exert anti-proliferative effects on HepG2 cells, we assessed cell proliferation following 3 days (9 h) of exposure and did not find any significant difference between cells exposed to HCC-specific modulation frequencies and unexposed cells (Figure 2B).

Further, to determine whether the growth-inhibitory effect of HCC-specific modulation frequencies persists over time and results in a decrease in the total number of tumour cells, we counted the number of HepG2 cells following treatment with HCC-specific modulation frequencies and that of untreated HepG2 cells weekly for up to 7 weeks. Cells that were either exposed to HCC-specific modulation frequencies or not exposed were split weekly at the same ratio over a period of 7 weeks. As shown in Figure 2C, when compared with unexposed HepG2 cells, the number of HepG2 cells following exposure to HCC-specific modulation frequencies decreased steadily over 7 weeks, resulting in a cumulative loss of 1.71×10^6 cells per ml at week 7.

The average specific absorption rate (SAR) for cells exposed in the parallel capacitor plate system is 0.03 W kg^{-1} (Supplementary Information). All initial experiments conducted with the TEM system were conducted at a SAR of 0.4 W kg^{-1}. To determine the range of SARs within which significant GI was observed, additional cell proliferation experiments were performed at 0.05, 0.1 and 1.0 W kg^{-1}. A significant anti-proliferative effect was observed at all SARs ranging from 0.05 to 1.0 W kg^{-1} ($P = 0.0354$). All subsequent assays with the TEM system were conducted at an SAR of 0.4 W kg^{-1}.

Inhibition of cell proliferation is tumour and tissue specific

Our previous clinical observations revealed that patients with HCC had biofeedback responses to specific modulation frequencies that were different from those identified in patients with other types of cancer, such as breast cancer (Barbault *et al*, 2009). To experimentally assess the relevance of these findings on the proliferation of tumour cells, we determined the specificity of frequencies identified in patients with these two tumour types given the documented objective clinical responses that included one complete and one partial response in two patients with metastatic breast cancer (Barbault *et al*, 2009) and three partial and one near-complete responses in four patients with HCC (Costa *et al*, 2011). A total of 194 breast cancer-specific modulation frequencies ranging in the same modulation frequency band from

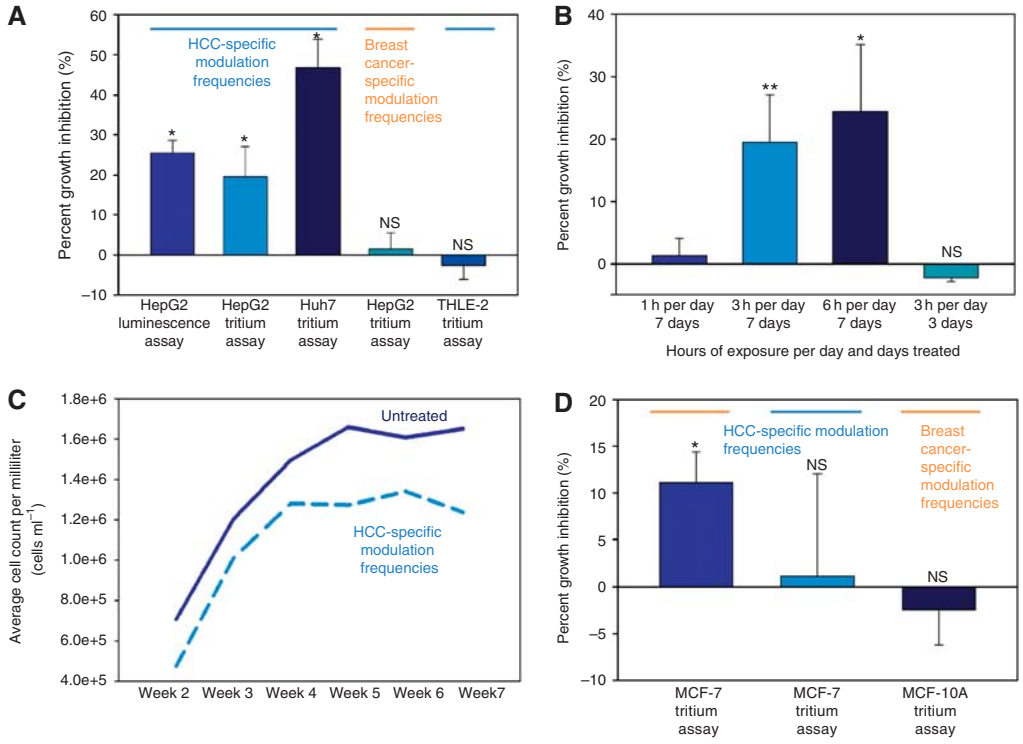

Figure 2 Cell proliferation assays of cell lines exposed to HCC-specific or breast cancer-specific modulation frequencies. (**A**) Cells were not split after initial seeding; medium was exchanged every 48 h. Experiments were performed with both equipment setups. Left to right columns: (1) HepG2 cells exposed to HCC-specific modulation frequencies with GI evaluated with a luminescence assay, 25.46 ± 3.22% GI ($P = 0.0009$). (2) HepG2 cells exposed to HCC-specific modulation frequencies with GI evaluated using tritium incorporation, 19.44 ± 7.60% GI ($P = 0.00993$). (3) Huh7 cells exposed to HCC-specific modulation frequencies, 47.73 ± 7.14% GI ($P = 0.018$). (4) HepG2 cells are not significantly inhibited when exposed to breast cancer-specific modulation frequencies, 1.49 ± 3.99% GI ($P = 0.8815$). (5) THLE-2 cells are not affected by HCC-specific modulation frequencies, −2.54 ± 3.54% GI ($P = 0.6550$). Values represent average percent GI ($n = 6$) ± %STERR. (**B**) Cell proliferation assays exposing cells for varying hours per day. Left to right: 1 h per day 1.36 ± 2.77% ($P = 0.8508$); 3 h per day 19.44 ± 7.60% ($P = 0.0099$); 6 h per day 24.46 ± 10.75% ($P = 0.0301$); 3 h per day for 3 days −2.12 ± 0.66% ($P = 0.4067$). Values represent average percent GI ($n = 6$) ± %STERR. (**C**) Cumulative decrease in cell counts over time when HepG2 cells are exposed to HCC-specific modulation frequencies. Samples were subcultured by volume every 7 days (1 : 20 split by volume). Average total cells mL^{-1} per week: week 2: 7.07×10^5, 4.75×10^5; week 3: 1.20×10^6, 1.01×10^5; week 4: 1.50×10^5, 1.28×10^5; week 5: 1.66×10^5, 1.22×10^5; week 6: 1.61×10^6, 1.34×10^6; week 7: 1.65×10^6, 1.24×10^6 for untreated and treated samples, respectively. For the duration of the 7-week experiment with time considered as a covariate: $P = 0.005751$. (**D**) Left to right columns: (1) MCF-7 cells exposed to breast tumour-specific modulation frequencies, 11.08 ± 3.30% GI ($P = 0.0230$). (2) MCF-7 cells are not significantly inhibited when exposed to HCC-specific modulation frequencies, 1.49 ± 3.99% ($P = 0.8815$) GI, respectively. (3) MCF-10A cells are not affected by breast tumour-specific modulation frequencies, −2.46 ± 3.75% GI ($P = 0.8579$). Values represent average percent GI ($n = 6$) ± %STERR.

100 Hz to 21 kHz have been identified in patients with a diagnosis of breast cancer (Supplementary Table 3). In all 9 (4.6%) of the HCC-specific modulation frequencies are identical to breast cancer-specific modulation frequencies.

The two patients with metastatic breast cancer who had experienced an objective response to breast cancer-specific modulation frequencies had tumours that over-expressed oestrogen receptor (ER+) and progesterone receptor (PR+), but did not over-express ERBB2 (ERBB2−) (Barbault *et al*, 2009). We therefore chose the MCF-7 cell line as it represents the same tumour phenotype, that is, ER+, PR+, ERBB2−. Although the growth of MCF-10A breast cells was unaffected by exposure to breast cancer-specific modulation frequencies, exposure of MCF-7 breast cancer cells to breast cancer-specific modulation frequencies significantly inhibited cell proliferation (Figure 2D). However, exposure of HepG2 cells to the same breast cancer-specific modulation frequencies did not affect cell proliferation (Figure 2A). Similarly, the proliferation of MCF-7 cells was not affected by exposure to HCC-specific modulation frequencies (Figure 2D). Consequently, the observed anti-proliferative effect on HCC and breast cancer cells was observed only upon exposure to tumour-specific modulation frequencies previously identified in patients with a diagnosis of HCC and breast cancer, respectively, despite the fact that more than 57% of the modulation frequencies only differed by <1% (Supplementary Tables 1 and 3).

Having demonstrated that the anti-proliferative effect of amplitude-modulated frequencies was tumour specific, we sought to determine whether the HCC-specific modulation frequencies have an effect on the proliferation of THLE-2 normal hepatocytes. As shown in Figure 2A, exposure of THLE-2 cells to HCC-specific modulation frequencies did not have any measurable effect on cell proliferation. These findings provide strong support for the novel notion that a combination of narrowly defined, specific modulation frequencies identified in a group of patients with the same type of cancer is capable of inhibiting cell proliferation in a tumour- and tissue-specific fashion.

Tumour-specific modulation frequencies and gene regulation

To study the mechanism by which tumour-specific modulation frequencies inhibit cell proliferation, we assessed the gene expression profile of HepG2 cells exposed to HCC-specific modulation frequencies using RNA-seq, as it provides a more

comprehensive assessment of differential gene expression across a broader range of expression levels than microarray-based analysis (Wang *et al*, 2009). Overall, we did not observe statistically significant differences in transcript levels when comparing two HepG2 cultures exposed for 1 week, 3 h a day to HCC-specific modulation frequencies with two HepG2 cultures exposed to randomly chosen modulation frequencies (Supplementary Figure 1). However, we did observe a small number of genes with an absolute fold-change >1.5 and a minimum mean RPKM of 1.5 following exposure to HCC-specific modulation frequencies. Two genes with an absolute fold-change >1.8 appeared to be downregulated in HepG2 cells exposed to HCC-specific modulation frequencies, *PLP2* and *XCL2*, and were considered to be candidates worthy of further experiments. We validated the downregulation of *PLP2* and *XCL2* with quantitative PCR in both HepG2 as well as Huh7 cells exposed to HCC-specific modulation frequencies (Figures 3A and B). There was no significant downregulation of *PLP2* and *XCL2* in MCF-7 breast cancer cells (Figure 3C). Similarly, there was no downregulation of *PLP2* and *XCL2* in nonmalignant cells, that is, in THLE-2 normal hepatocytes (Figure 3D), or in lymphoblastoid cell lines from healthy individuals (Figures 3E and F). These findings support the novel notion that the demodulation effects of RF EMF amplitude-modulated at specific frequencies inhibit cell proliferation and affect the expression of several genes in a tumour- and tissue-specific fashion.

Tumour-specific modulation frequencies and disruption of the mitotic spindle

There is evidence that the proliferation of several rodent and human cancer cell lines is arrested by exposure to sinusoidal electric fields of 100–200 V m^{-1} at a frequency of 100–300 kHz (Kirson *et al*, 2004). This approach has also shown efficacy in animal and human tumour models as well as promising results in the treatment of patients with cancer (Kirson *et al*, 2004; Kirson *et al*, 2007; Salzberg *et al*, 2008; Kirson *et al*, 2009). The antitumour effect of this therapeutic approach appears to be caused by disruption of the mitotic spindle mediated by interference of spindle tubulin orientation and induction of dielectrophoresis (Kirson *et al*, 2004; Kirson *et al*, 2007). In contrast to the sinusoidal signals (Kirson *et al*, 2004), the carrier frequency of the signal applied in our experiments is more than 100 times higher; the peak E-field amplitude of the carrier at 0.4 W kg^{-1} corresponds to approximately 35 V m^{-1} inside the cell medium when the signal is sinusoidally amplitude-modulated at specific frequencies with 85% modulation depth (Kirson *et al*, 2004).

Despite these significant differences, confocal laser scanning microscopy revealed pronounced disruption of the mitotic spindle in more than 60% of HepG2 cells exposed for 1 week, 3 h per day to HCC-specific modulation frequencies whereas there was no disruption of the mitotic spindle in unexposed HepG2 cells (Figures 4A and B). Specifically, the observed cytoskeletal disruption in cells exposed to HCC-specific modulation frequencies was apparent in cells in mitosis, in which we saw centrosomal distortion and poor chromosomal separation at anaphase (Figure 4D). We found no evidence of karyotypic differences between HepG2 cells exposed to HCC-specific modulation frequencies and unexposed HepG2 cells.

DISCUSSION

By exposing HCC cells to 27.12 MHz RF EMF sinusoidally amplitude-modulated at specific frequencies, which were previously

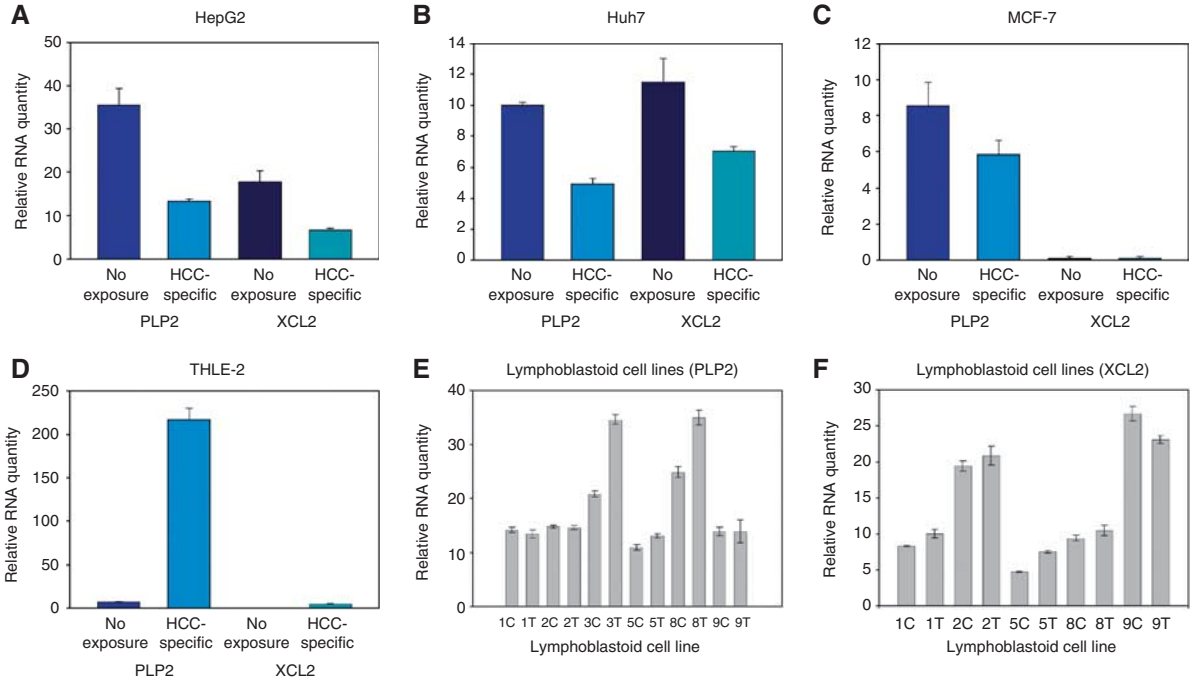

Figure 3 Expression of *XCL2* and *PLP2* receiving HCC-specific RF EMF compared with cells not receiving exposure. (**A**) HepG2: *PLP2* (35.46 ± 3.85; 13.17 ± 0.70) and *XCL2* (17.87 ± 2.49; 6.52 ± 0.48) ($P = 9.0371e\text{-}3$ and $P = 0.0179$, respectively). (**B**) Huh7: *PLP2* (10.02 ± 0.19; 4.95 ± 0.35) and *XCL2* (11.52 ± 1.49; 7.02 ± 0.29) ($P = 9.4981e\text{-}5$ and $P = 0.0536$, respectively). (**C**) MCF-7: *PLP2* (8.52 ± 1.30; 5.84 ± 0.77) and *XCL2* (levels not detectable). (**D**) THLE-2: *PLP2* (7.11 ± 0.14; 216.89 ± 13.18) and *XCL2* (0.03 ± 0.01; 4.55 ± 1.04) in THLE-2 cells exposed to HCC-specific modulation frequencies ($P = 5.5108e\text{-}4$ and $P = 0.0221$, respectively). (**E**) Expression levels of *PLP2* in lymphoblastoid cell lines (C = unexposed; T = HCC-specific exposure) (for all cell lines compiled $P = 0.418$), LCL 3 expression was significant $P = 0.0021$ as was LCL8 $P = 0.0159$ (**F**) Expression levels of *XCL2* in lymphoblastoid cell lines (for all cell lines compiled ($P = 0.899$), LCL 1 expression difference was significant $P = 0.0002$. Values represent average relative RNA expression ($n = 4$) ± s.e.m. Levels were normalised to levels of GAPDH.

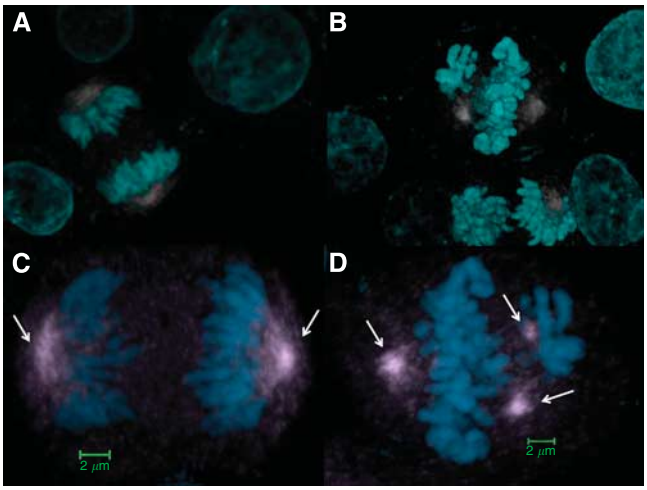

Figure 4 Mitotic spindle disruption in cells receiving HCC-specific RF EMF compared with cells not receiving exposure. (**A**) HepG2 efficiently assembles a bipolar mitotic spindle, allowing cells to pass through the mitotic assembly checkpoint and successfully progress from metaphase to anaphase, (**B**) >60% of dividing HepG2 cells exposed to HCC-specific modulation frequencies exhibit microtubule-associated anomalies, (**C**) high magnification of unexposed HepG2 cells in mitosis (**D**) high magnification of HepG2 cells exposed to HCC-specific modulation frequencies shows errors such as tripolar spindle formation (Cyan = DAPI; Gray = Microtubules; Arrows = mitotic spindle).

identified in patients with a diagnosis of HCC (Barbault *et al*, 2009) and result in therapeutic responses in patients with HCC (Costa *et al*, 2011), we demonstrate a robust and sustained anti-proliferative effect. This effect was seen within SARs ranging from 0.03 to 1.0 W kg^{-1}, that is, within the range of exposure in humans receiving treatment administered intrabuccally (Barbault *et al*, 2009; Costa *et al*, 2011). HCC-specific modulation frequencies began to hinder cell proliferation after 7 days of exposure and the anti-proliferative effect increased over a 7-week period. The anti-proliferative effect HCC-specific modulation frequencies were observed only in HCC cells, but not in breast cancer cells or normal hepatocytes.

The specificity of modulation frequencies is exemplified by the fact that two sets of similar modulation frequencies (breast cancer-specific and randomly chosen) within the same range, that is, from 100 Hz to 21 kHz, did not affect the proliferation of HCC cells. Similarly, the proliferation of breast cancer cells was affected only by breast cancer-specific modulation frequencies, but neither by HCC-specific nor by randomly chosen modulation frequencies. The fact that >50% of the modulation frequencies from these three programs differed by <1%, provides strong experimental evidence that the biological effects are only mediated by a combination of narrowly defined, tumour-specific modulation frequencies.

The modulation-frequency specific laboratory findings are consistent with the clinical observation of a complete response in a patient with breast cancer metastatis to the adrenal gland and the bone while a primary malignancy of the uterus continued to grow (Barbault *et al*, 2009). This suggests that a combination of precise tumour-specific modulation frequencies is needed to block cancer growth *in vitro* and in patients with a diagnosis of cancer. The clinical results reported by Barbault *et al*, (2009) and Costa *et al*, (2011) as well as laboratory evidence included in this report provide support for the novel and transformational concept that the growth of human tumours arising from the same primary tissue may be effectively blocked by identical modulation frequencies. While receiving treatment with HCC-specific modulation frequencies, one black and three white patients with advanced carcinoma had partial responses (Costa *et al*, 2011). Furthermore, proliferation of the Huh7 HCC cell line, which is derived from a Japanese patient's tumour (Nakabayashi *et al*, 1982), exhibited the most pronounced response to HCC-specific modulation frequencies (Figure 2A). This indicates that the frequency signature and biological effects of HCC-specific modulation frequencies are likely independent of ethnic status.

There is no known biophysical mechanism accounting for the effect observed in these experiments; however, other modulation-frequency dependent effects have been observed in biological systems at similarly low exposure levels. Documented effects have occurred in cellular processes controlling cell growth, proliferation, and differentiation (Blackman, 2009). Further, modulation of the signal appears to be a critical factor in the response of biological systems to electromagnetic fields (Blackman, 2009). The amount of electromagnetic energy delivered is far too low to break chemical bonds or cause thermal effects, necessitating alternative mechanistic explanations for observed biological outcomes. Several theories have been put forth to explain biological responses to electromagnetic fields. Some reports have shown that low levels of electromagnetic fields can alter gene expression and subsequent protein synthesis by interaction of the electromagnetic field with specific DNA sequences within the promoter region of genes (Blank and Goodman, 2008; Blank and Goodman, 2009). Such changes have been demonstrated in the family of 'heat shock' proteins that function in the cell stress response (Blank and Goodman, 2009).

To thoroughly interrogate gene expression changes in cells exhibiting decreased cell proliferation, we used high-throughput sequencing technologies to sequence the cells' cDNA, a technique that has become invaluable in the study of cancer (Maher *et al*, 2009). Tumour cell GI was associated with downregulation of *PLP2* and *XCL2* as well as with disruption of the mitotic spindle. *PLP2* encodes an integral membrane protein that localises to the endoplasmic reticulum in epithelial cells. The encoded protein can multimerise and may function as an ion channel (Breitwieser *et al*, 1997). *PLP2* enhances chemotaxis of human osteogenic sarcoma cells (Lee *et al*, 2004) and *PLP2* downregulation is associated with decreased metastasis in a mouse model of cancer (Sonoda *et al*, 2010). *XCL2* encodes for a protein that enhances chemotactic activity for lymphocytes and downregulation of *XCL2* has been shown to be associated with good prognosis in patients with breast cancer (Teschendorff *et al*, 2007; Teschendorff and Caldas, 2008). The pronounced disruption of the mitotic spindle seen in the majority of HepG2 cells exposed to HCC-specific modulation frequencies undergoing mitosis is not associated with karyotypic changes, but may be a major determinant of the anti-tumour effects of HCC-specific modulation frequencies accounting for the therapeutic responses seen in patients receiving the same modulation frequencies (Costa *et al*, 2011).

Exposure of HCC cells to the same RF EMF modulated at slightly different modulation frequencies did not result in changes in gene expression, which demonstrates that inhibition of cell proliferation is associated with changes in gene expression levels.

In conclusion, we show that very low levels of 27.12 MHz radiofrequency electromagnetic fields, which are comparable to the levels administered to patients, inhibit tumour cell growth when modulated at specific frequencies. The exciting findings presented in this report suggest that the anti-proliferative effect of modulation frequencies is both tumour- and tissue-specific, and is mediated by changes in gene expression as well as disruption of the mitotic spindle. These findings uncover a new alley to control tumour growth and may have broad implications for the treatment of cancer.

ACKNOWLEDGEMENTS

We thank Dr Carl F. Blackman, 3413 Horton Street, Raleigh, NC, Dr Richard B. Marchase, UAB, and Dr Bernard Veyret, University of Bordeaux for reviewing the manuscript. We also thank Dr Andrew Carroll, Cytogenetics Laboratory, UAB Department of Genetics, for performing the karyotype analysis. We would also like to thank Dr Jeff Edberg for the lymphoblastoid cell lines from the UAB Control Population. Finally, we would like to thank Dr Nareej Saxena, Emory University for his expertise and the gift of Huh7 cells.

Supplementary Information accompanies the paper on British Journal of Cancer website (http://www.nature.com/bjc)

REFERENCES

Barbault A, Costa F, Bottger B, Munden R, Bomholt F, Kuster N, Pasche B (2009) Amplitude-modulated electromagnetic fields for the treatment of cancer: discovery of tumor-specific frequencies and assessment of a novel therapeutic approach. *J Exp Clin Cancer Res* **28**(1)**:** 51

Blackman C (2009) Cell phone radiation: evidence from ELF and RF studies supporting more inclusive risk identification and assessment. *Pathophysiology* **16:** 205 – 216

Blank M, Goodman R (2008) A mechanism for stimulation of biosynthesis by electromagnetic fields: charge transfer in DNA and base pair separation. *J Cell Physiol* **214:** 20 – 26

Blank M, Goodman R (2009) Electromagnetic fields stress living cells. *Pathophysiology* **16:** 71 – 78

Breitwieser GE, McLenithan JC, Cortese JF, Shields JM, Oliva MM, Majewski JL, Machamer CE, Yang VW (1997) Colonic epithelium-enriched protein A4 is a proteolipid that exhibits ion channel characteristcs. *Am J Physiol* **272**(3 Pt 1)**:** C957 – C965

Brothman AR, Persons DL, Shaffer LG (2009) Nomenclature evolution: changes in the ISCN from the 2005 to the 2009 edition. *Cytogenet Genome Res* **127:** 1 – 4

Costa FP, de Oliveira AC, Meirelles R, Machado MCC, Zanesco T, Surjan R, Chammas MC, de Souza Rocha M, Morgan D, Cantor A, Zimmerman J, Brezovich I, Kuster N, Barbault A, Pasche B (2011) Treatment of advanced hepatocellular carcinoma with very low levels of amplitude-modulated electromagnetic fields. *Br J Cancer* **105**(5)**:** 640 – 648

Kirson ED, Dbaly V, Tovarys F, Vymazal J, Soustiel JF, Itzhaki A, Mordechovich D, Steinberg-Shapira S, Gurvich Z, Schneiderman R, Wasserman Y, Salzberg M, Ryffel B, Goldsher D, Dekel E, Palti Y (2007) Alternating electric fields arrest cell proliferation in animal tumor models and human brain tumors. *PNAS* **104**(24)**:** 10152 – 10157

Kirson ED, Giladi M, Gurvich Z, Itzhaki A, Mordechovich D, Schneiderman RS, Wasserman Y, Ryffel B, Goldsher D, Palti Y (2009) Alternating electric fields (TTFields) inhibit metastatic spread of solid tumors to the lungs. *Clin Exp Metastasis* **26**(7)**:** 633 – 640.

Kirson ED, Gurvich Z, Schneiderman R, Dekel E, Itzhaki A, Wasserman Y, Schatzberger R, Palti Y (2004) Disruption of cancer cell replication by alternating electric fields. *Cancer Res* **64**(9)**:** 3288 – 3295

Lee SM, Shin H, Jang SW, Shim JJ, Song IS, Son KN, Hwang J, Shin YH, Kim HH, Lee CK, Ko J, Na DS, Kwon BS, Kim J (2004) PLP2/A4 interacts with CCR1 and stimulates migration of CCR1-expressing HOS cells. *Biochem Biophys Res Commun* **324:** 768 – 772

Maher CA, Kumar-Sinha C, Cao X, Kalyana-Sundaram S, Han B, Jing X, Sam L, Barrette T, Palanisamy N, Chinnaiyan AM (2009) Transcriptome sequencing to detect gene fusions in cancer. *Nature* **458**(7234)**:** 97 – 101, doi:10.1038/nature07638

Nakabayashi H, Taketa K, Miyano K, Yamane T, Sato J (1982) Growth of human hepatoma cell lines with differentiated functions in chemically defined medium. *Cancer Res* **42:** 3858 – 3863

Reddy TE, Pauli F, Sprouse RO, Neff NF, Newberry KM, Garabedian MJ, Myers RM (2009) Genomic determination of the glucocorticoid response reveals unexpected mechanisms of gene regulation. *Genome Res* **19**(12)**:** 2163 – 2171

Rosman DS, Phukan S, Huang CC, Pasche B (2008) TGFBR1*6A enhances the migration and invasion of MCF-7 breast cancer cells through RhoA activation. *Cancer Res* **68**(5)**:** 1319 – 1328

Salzberg M, Kirson E, Palti Y, Rochlitz C (2008) A pilot study with very low-intensity, intermediate-frequency electric fields in patients with locally advanced and/or metastatic solid tumors. *Onkologie* **31**(7)**:** 362 – 365.

Sonoda Y, Warita M, Suzuki T, Ozawa H, Fukuda Y, Funakoshi-Tago M, Kasahara T (2010) Proteolipid protein 2 is associated with melanoma metastasis. *Oncol Rep* **23:** 371 – 376

Teschendorff AE, Caldas C (2008) A robust classifier of high predictive value to identify good prognosis patients in ER-negative breast cancer. *Breast Cancer Res* **10**(4)**:** R73.

Teschendorff AE, Miremadi A, Pinder SE, Ellis IO, Caldas C (2007) An immune response gene expression module identifies a good prognosis subtype in estrogen receptor negative breast cancer. *Genome Biol* **8**(8)**:** R157.

Thomas MB, Zhu AX (2005) Hepatocellular carcinoma: the need for progress. *J Clin Oncol* **23**(13)**:** 2892 – 2899

Wang Z, Gerstein M, Snyder M (2009) RNA-Seq: a revolutionary tool for transcriptomics. *Nat Rev Genet* **10:** 57 – 63

Supplementary notes

1 Design and construction of *in vitro* exposure devices

1.1 Exposure system connected to the same devices as those use for clinical studies. An apparatus for cell irradiation was designed and built to expose cell cultures to the same radiofrequency (RF) signal as the one used for treatment of patients. Briefly, the design of four identical exposure chambers is based on a parallel plate capacitor (14 x 21 cm) arrangement excited by devices identical to the ones used for clinical studies (the outer two plates on the device ground and the center plate on the active port to establish symmetry) (Figure 1A). The outer brass plates are connected to the outer conductor of the coaxial cable, whereas the center brass plate is connected to the inner conductor of the coaxial cable. Connections are made near the middle of the narrow edges of the plates (Figure 1A).

One set of devices is programmed with the same HCC-specific or breast cancer-specific frequencies as those used for patient treatment (Suppl. Tables 1 and 3, Suppl. Figure 2). Another set of devices is programmed with randomly-chosen frequencies selected in the same band as the HCC-specific frequencies, i.e. from 100 Hz to 21 kHz (Suppl. Table 2, Suppl. Figure 2). Additional control devices consisted of the same devices, which were not switched on. Temperature of the culture medium was measured before and after treatment. There was no measurable difference in the temperature of the media during and following exposure to amplitude-modulated frequencies in the parallel plate capacitor. The averaged induced SAR at the monolayer was assessed to be 0.034 W/kg (uncertainty of 40%) and a standard deviation of 155% (highest cell exposures at the edge of the dish and smallest exposures in the center).

1.2 sXc27 TEM System. An optimized system for well controlled exposure of cell cultures to 27.12 MHz radiofrequency (RF) electromagnetic fields was developed, manufactured, and characterized by the Foundation for Research in Information Technologies in Society (IT'IS Foundation, Zurich, Switzerland). The system is based on two identical transverse electromagnetic (TEM) cells (IFI CC110, Instruments for Industry Inc., Ronkonkoma N.Y.) that can be loaded with 2 x 6 tissue culture dishes (35 mm, FALCON, monolayer cells) (Figure 1B). The dish holder is made out of polyoxymethylene (POM, relative permittivity = 3.5 (50%) conductivity = 0.0001 (50%) at the 27 MHz and 37°C). The design is an adaptation of the system described by Nikoloski et al.(2005). The propagation vector is normal to the bottom of the tissue culture dish allowing homogenous exposure of cell monolayers and cells in suspension. A constant airflow is forced through the system by fans with a common inlet ensuring the same environmental conditions as inside the incubator. The controlling and monitoring unit generates the exposure signal via computer-controlled signal generators and monitors the exposure levels using power sensors at the output of the TEM cells. It also monitors temperature and the functioning of the fans every 5s. All measured and control parameters are stored in a log file. Since the system consists of two identical chambers, it allows blinded exposure schemes with active and inactive RF-modulations, i.e. the computer randomly selects the active versus inactive signals, the information of which is only accessible via the log file.

The specific absorption rate (SAR) distribution within the cell culture dish was characterized with the electromagnetic and thermal simulation platform SEMCAD X V14 that was developed by the IT'IS Foundation and SPEAG (Zurich, Switzerland) (Figure 1C). The results of the simulations were validated by measurements using temperature probes T1V3lab (SPEAG, Zurich).

The efficiency of the exposure system for the cell monolayer is 10.7 mW/kg per Watt of forward

power for the MCF-7 medium (relative permittivity = 75 (2.5%), conductivity = 1.66 (5%) at the 27 MHz and 37°C) and 10.2 mW/kg for the HepG2 medium (relative permittivity = 74.3 (2.5%), conductivity = 1.74 (5%) at the 27 MHz and 37°C). The variation of averaged SAR between the six tissue culture dishes is less than +/-8% (Figure 1C). The non-uniformity of the cell monolayer exposure is 19% (SD, k=1) for all dishes. The maximum possible temperature increase inside the cell medium due to RF exposure is < 0.1°C per W/kg averaged exposure. The combined relative uncertainty for the whole dosimetric assessment is 23%, and SAR variability between experiments is ≤ 6%. Temperature difference in the sXc27 system between exposed and unexposed was less than 0.04°C at 0.4 W/kg.

Reference List

1. Nikoloski N, Frohlich J, Samaras T, Schuderer J, Kuster N (2005) Reevaluation and improved design of the TEM cell in vitro exposure unit for replication studies. *Bioelectromagnetics* **26**(3):215-224.

Supplementary Figure 1

RNA-Seq assay of HepG2 cells exposed to HCC-specific vs. randomly chosen modulation frequencies.

Supplementary Figure 2

Graphical representation of the HCC-specific, randomly-chosen and breast cancer-specific frequencies.

Frequencies are located in the 100 Hz to 21 kHz band.

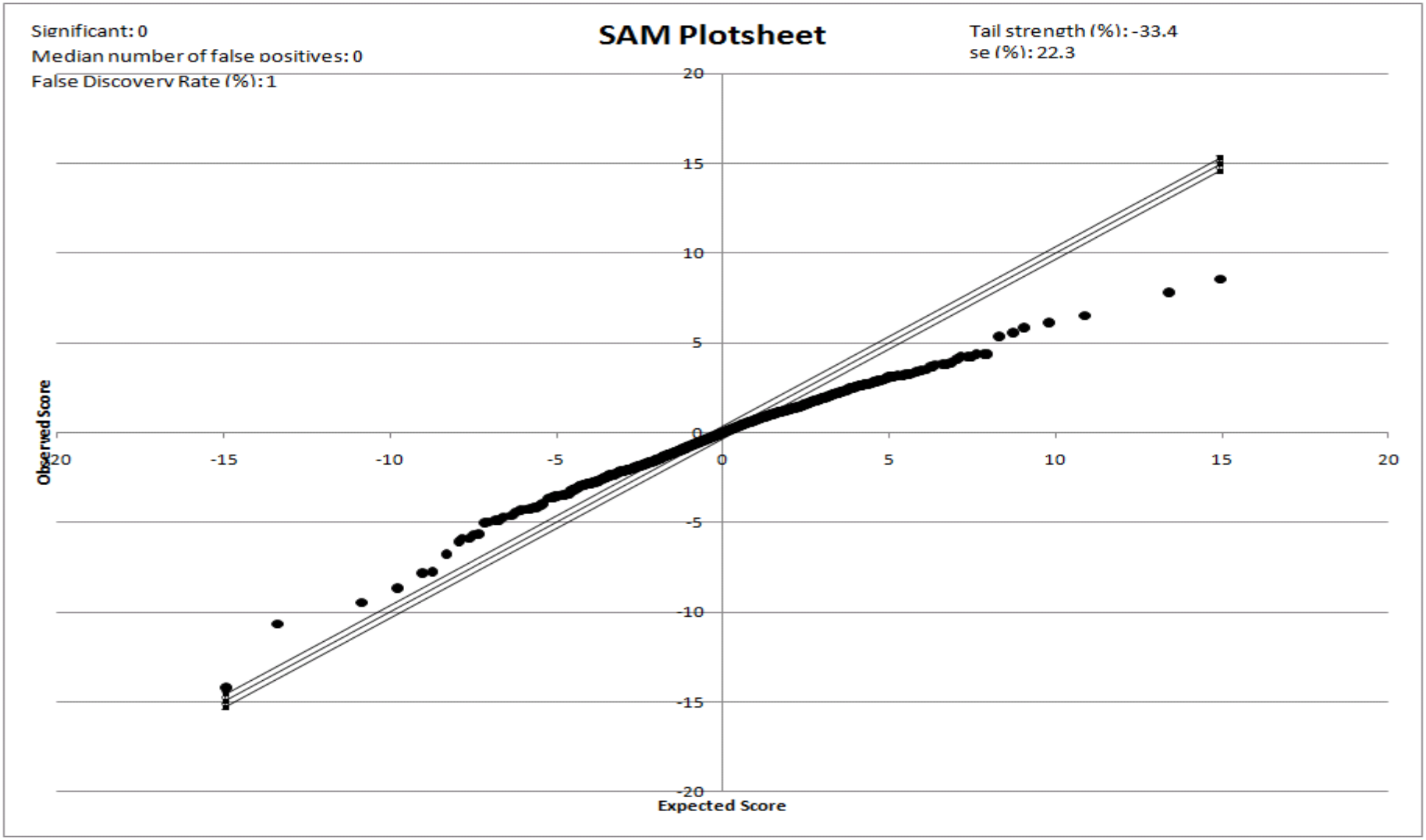
Significant: 0
Median number of false positives: 0
False Discovery Rate (%): 1
SAM Plotsheet
Tail strength (%): -33.4
se (%): 22.3
Observed Score
Expected Score
20
15
10
5
0
-5
-10
-15
-20
-20
-15
-10
-5
0
5
10
15
20

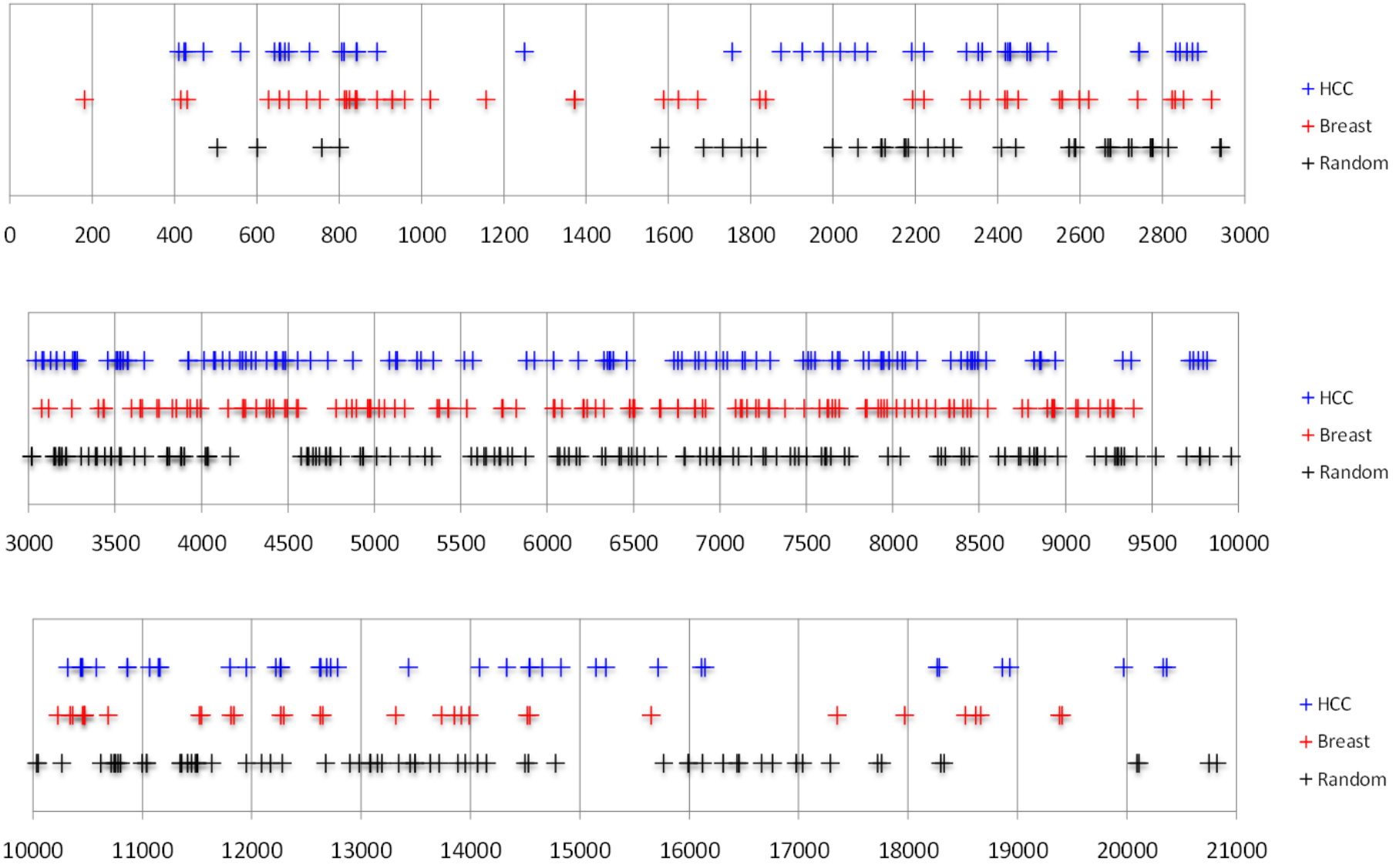
HCC
Breast
Random
0
200
400
600
800
1000
1200
1400
1600
1800
2000
2200
2400
2600
2800
3000
HCC
Breast
Random
3000
3500
4000
4500
5000
5500
6000
6500
7000
7500
8000
8500
9000
9500
10000
HCC
Breast
Random
10000
11000
12000
13000
14000
15000
16000
17000
18000
19000
20000
21000

Supplementary Table 1

HCC-specific modulation frequencies

Number	Frequency
1	410.231 Hz
2	423.321 Hz
3	427.062 Hz
4	470.181 Hz
5	560.32 Hz
6	642.932 Hz
7	655.435 Hz
8	657.394 Hz
9	668.209 Hz
10	677.972 Hz
11	728.232 Hz
12	806.021 Hz
13	811.924 Hz
14	842.311 Hz
15	843.22 Hz
16	891.901 Hz
17	1250.504 Hz
18	1755.402 Hz
19	1873.477 Hz
20	1924.702 Hz
21	1975.196 Hz
22	2017.962 Hz
23	2053.396 Hz
24	2083.419 Hz
25	2190.731 Hz
26	2221.323 Hz
27	2324.393 Hz
28	2353.478 Hz
29	2362.309 Hz
30	2419.309 Hz
31	2425.222 Hz
32	2430.219 Hz
33	2431.094 Hz
34	2471.328 Hz
35	2478.331 Hz
36	2480.191 Hz
37	2522.328 Hz
38	2743.995 Hz
39	2744.211 Hz
40	2831.951 Hz
41	2843.283 Hz

42	2859.891 Hz
43	2873.542 Hz
44	2886.232 Hz
45	3042.012 Hz
46	3078.983 Hz
47	3086.443 Hz
48	3127.232 Hz
49	3160.942 Hz
50	3161.331 Hz
51	3206.315 Hz
52	3255.219 Hz
53	3267.433 Hz
54	3269.321 Hz
55	3281.432 Hz
56	3457.291 Hz
57	3505.229 Hz
58	3516.296 Hz
59	3530.188 Hz
60	3531.296 Hz
61	3546.323 Hz
62	3572.106 Hz
63	3576.189 Hz
64	3669.513 Hz
65	3923.221 Hz
66	3927.331 Hz
67	4013.932 Hz
68	4071.121 Hz
69	4079.951 Hz
70	4123.953 Hz
71	4161.889 Hz
72	4222.821 Hz
73	4238.402 Hz
74	4256.321 Hz
75	4289.296 Hz
76	4312.947 Hz
77	4375.962 Hz
78	4426.387 Hz
79	4435.219 Hz
80	4471.188 Hz
81	4483.889 Hz
82	4486.384 Hz
83	4556.322 Hz
84	4629.941 Hz
85	4732.211 Hz

86	4876.218 Hz
87	5086.281 Hz
88	5124.084 Hz
89	5133.121 Hz
90	5247.142 Hz
91	5270.834 Hz
92	5340.497 Hz
93	5520.218 Hz
94	5570.234 Hz
95	5882.292 Hz
96	5926.512 Hz
97	6037.311 Hz
98	6180.334 Hz
99	6329.195 Hz
100	6350.333 Hz
101	6361.321 Hz
102	6364.928 Hz
103	6383.321 Hz
104	6461.175 Hz
105	6733.331 Hz
106	6758.232 Hz
107	6779.482 Hz
108	6856.222 Hz
109	6877.183 Hz
110	6915.886 Hz
111	6980.525 Hz
112	7019.235 Hz
113	7043.209 Hz
114	7130.323 Hz
115	7144.142 Hz
116	7210.223 Hz
117	7291.21 Hz
118	7482.245 Hz
119	7510.92 Hz
120	7529.233 Hz
121	7549.212 Hz
122	7650.028 Hz
123	7680.518 Hz
124	7692.522 Hz
125	7829.231 Hz
126	7862.209 Hz
127	7932.482 Hz
128	7935.423 Hz
129	7947.392 Hz

130	7979.308 Hz
131	8028.339 Hz
132	8055.942 Hz
133	8072.134 Hz
134	8141.174 Hz
135	8336.383 Hz
136	8394.793 Hz
137	8432.181 Hz
138	8452.119 Hz
139	8460.944 Hz
140	8475.221 Hz
141	8492.193 Hz
142	8542.311 Hz
143	8818.104 Hz
144	8852.329 Hz
145	8853.444 Hz
146	8858.179 Hz
147	8939.212 Hz
148	9332.397 Hz
149	9381.221 Hz
150	9719.314 Hz
151	9740.219 Hz
152	9768.331 Hz
153	9797.294 Hz
154	9819.511 Hz
155	10317.499 Hz
156	10438.495 Hz
157	10443.311 Hz
158	10456.383 Hz
159	10579.425 Hz
160	10863.209 Hz
161	10866.382 Hz
162	11067.418 Hz
163	11149.935 Hz
164	11163.895 Hz
165	11802.821 Hz
166	11953.424 Hz
167	12223.329 Hz
168	12260.933 Hz
169	12265.295 Hz
170	12267.233 Hz
171	12623.191 Hz
172	12633.372 Hz
173	12685.231 Hz

174	12721.423 Hz
175	12785.342 Hz
176	13433.323 Hz
177	14085.222 Hz
178	14333.209 Hz
179	14537.331 Hz
180	14542.432 Hz
181	14655.03 Hz
182	14828.234 Hz
183	15149.213 Hz
184	15237.489 Hz
185	15717.221 Hz
186	16110.932 Hz
187	16144.343 Hz
188	18265.238 Hz
189	18283.323 Hz
190	18863.292 Hz
191	18930.995 Hz
192	19970.311 Hz
193	20330.294 Hz
194	20365.284 Hz
195	

Supplementary Table 2

Randomly-chosen modulation frequencies

Number	Frequency
1	504.288 Hz
2	601.388 Hz
3	758.079 Hz
4	801.055 Hz
5	1579.861 Hz
6	1686.129 Hz
7	1732.231 Hz
8	1777.676 Hz
9	1816.165 Hz
10	1999.19 Hz
11	2060.824 Hz
12	2117.172 Hz
13	2118.13 Hz
14	2126.078 Hz
15	2172.715 Hz
16	2177.378 Hz
17	2182.699 Hz
18	2230.497 Hz
19	2270.095 Hz
20	2291.76 Hz
21	2409.804 Hz
22	2443.455 Hz
23	2573.901 Hz
24	2586.187 Hz
25	2588.825 Hz
26	2661.239 Hz
27	2667.744 Hz
28	2673.24 Hz
29	2674.203 Hz
30	2718.46 Hz
31	2726.164 Hz
32	2771.084 Hz
33	2774.56 Hz
34	2777.798 Hz
35	2814.508 Hz
36	2940.689 Hz
37	2942.388 Hz
38	3018.394 Hz
39	3018.632 Hz
40	3145.88 Hz
41	3154.706 Hz

Each modulation frequency is at least 0.4 Hz higher or lower than any HCC-specific (Suppl. Table 1) or breast cancer-specific (Suppl. Table 3) modulation frequencies.

42	3174.855 Hz
43	3177.169 Hz
44	3178.166 Hz
45	3191.69 Hz
46	3214.895 Hz
47	3218.57 Hz
48	3302.561 Hz
49	3346.213 Hz
50	3386.881 Hz
51	3395.087 Hz
52	3439.955 Hz
53	3477.036 Hz
54	3477.464 Hz
55	3526.946 Hz
56	3534.597 Hz
57	3612.538 Hz
58	3671.955 Hz
59	3800.538 Hz
60	3803.02 Hz
61	3814.561 Hz
62	3881.652 Hz
63	3883.206 Hz
64	3884.425 Hz
65	3900.955 Hz
66	4024.069 Hz
67	4035.5 Hz
68	4036.464 Hz
69	4037.745 Hz
70	4166.946 Hz
71	4577.652 Hz
72	4611.675 Hz
73	4619.808 Hz
74	4645.103 Hz
75	4662.242 Hz
76	4681.953 Hz
77	4718.225 Hz
78	4722.427 Hz
79	4743.75 Hz
80	4744.241 Hz
81	4806.447 Hz
82	4918.306 Hz
83	4932.277 Hz
84	4935.022 Hz
85	5013.21 Hz

86	5092.935 Hz
87	5205.432 Hz
88	5294.062 Hz
89	5333.86 Hz
90	5562.3 Hz
91	5594.909 Hz
92	5636.492 Hz
93	5646.433 Hz
94	5696.275 Hz
95	5725.188 Hz
96	5728.435 Hz
97	5771.856 Hz
98	5797.917 Hz
99	5874.546 Hz
100	6059.997 Hz
101	6072.239 Hz
102	6101.533 Hz
103	6127.257 Hz
104	6170.599 Hz
105	6189.464 Hz
106	6317.311 Hz
107	6338.888 Hz
108	6417.29 Hz
109	6429.727 Hz
110	6470.521 Hz
111	6489.2 Hz
112	6519.163 Hz
113	6562.089 Hz
114	6641.042 Hz
115	6794.29 Hz
116	6798.367 Hz
117	6885.025 Hz
118	6923.269 Hz
119	6962.114 Hz
120	6997.453 Hz
121	7001.42 Hz
122	7075.988 Hz
123	7107.292 Hz
124	7181.377 Hz
125	7250.347 Hz
126	7264.92 Hz
127	7327.056 Hz
128	7406.664 Hz

129	7434.055 Hz
130	7457.43 Hz
131	7502.744 Hz
132	7588.962 Hz
133	7606.907 Hz
134	7614.849 Hz
135	7642.973 Hz
136	7721.158 Hz
137	7747.529 Hz
138	7972.361 Hz
139	8045.29 Hz
140	8262.012 Hz
141	8282.156 Hz
142	8304.133 Hz
143	8399.157 Hz
144	8415.03 Hz
145	8443.098 Hz
146	8612.154 Hz
147	8648.429 Hz
148	8728.965 Hz
149	8742.131 Hz
150	8791.497 Hz
151	8817.564 Hz
152	8831.172 Hz
153	8837.559 Hz
154	8879.347 Hz
155	8955.291 Hz
156	9170.021 Hz
157	9234.272 Hz
158	9285.749 Hz
159	9297.33 Hz
160	9307.038 Hz
161	9322.743 Hz
162	9341.412 Hz
163	9410.744 Hz
164	9521.482 Hz
165	9699.914 Hz
166	9776.888 Hz
167	9779.743 Hz
168	9833.133 Hz
169	9960.676 Hz
170	10034.941 Hz
171	10047.505 Hz

172	10265.636 Hz
173	10622.538 Hz
174	10714.24 Hz
175	10745.164 Hz
176	10758.081 Hz
177	10777.023 Hz
178	10801.462 Hz
179	11000.996 Hz
180	11038.765 Hz
181	11040.509 Hz
182	11349.248 Hz
183	11360.871 Hz
184	11416.707 Hz
185	11449.28 Hz
186	11487.642 Hz
187	11502.021 Hz
188	11506.807 Hz
189	11637.367 Hz
190	11953.02 Hz
191	12089.99 Hz
192	12174.159 Hz
193	12280.284 Hz
194	12676.699 Hz
195	12899.888 Hz
196	12983.103 Hz
197	13083.597 Hz
198	13088.188 Hz
199	13148.766 Hz
200	13189.52 Hz
201	13345.41 Hz
202	13445.661 Hz
203	13491.824 Hz
204	13493.956 Hz
205	13634.291 Hz
206	13713.74 Hz
207	13885.51 Hz
208	13953.754 Hz
209	14063.876 Hz
210	14145.498 Hz
211	14499.838 Hz
212	14529.908 Hz
213	14776.655 Hz
214	15493.744 Hz

215	15766.529 Hz
216	15991.064 Hz
217	15996.675 Hz
218	16120.533 Hz
219	16311.057 Hz
220	16438.714 Hz
221	16454.99 Hz
222	16664.134 Hz
223	16761.237 Hz
224	16976.962 Hz
225	17037.895 Hz
226	17288.9437 Hz
227	17722.025 Hz
228	17758.777 Hz
229	18297.264 Hz
230	18328.755 Hz
231	20091.761 Hz
232	20111.655 Hz
233	20749.621 Hz
234	20824.094 Hz
235	21967.342 Hz
236	22363.323 Hz
237	22401.812 Hz
238	

Supplementary Table 3

Breast tumor-specific modulation frequencies

Number	Frequency
1	181.821 Hz
2	414.817 Hz
3	430.439 Hz
4	628.431 Hz
5	655.435 Hz
6	677.972 Hz
7	721.313 Hz
8	752.933 Hz
9	813.205 Hz
10	818.342 Hz
11	825.145 Hz
12	839.521 Hz
13	841.211 Hz
14	843.312 Hz
15	891.901 Hz
16	929.095 Hz
17	929.131 Hz
18	958.929 Hz
19	1021.311 Hz
20	1156.79 Hz
21	1372.207 Hz
22	1372.934 Hz
23	1588.721 Hz
24	1624.802 Hz
25	1670.699 Hz
26	1821.729 Hz
27	1836.219 Hz
28	2193.937 Hz
29	2221.323 Hz
30	2278.312 Hz
31	2332.949 Hz
32	2357.832 Hz
33	2417.323 Hz
34	2423.292 Hz
35	2450.332 Hz
36	2551.313 Hz
37	2556.221 Hz
38	2598.853 Hz
39	2621.322 Hz
40	2740.191 Hz

41	2823.428 Hz
42	2831.386 Hz
43	2851.347 Hz
44	2919.273 Hz
45	3074.333 Hz
46	3115.188 Hz
47	3249.529 Hz
48	3405.182 Hz
49	3432.274 Hz
50	3434.693 Hz
51	3594.231 Hz
52	3647.619 Hz
53	3657.931 Hz
54	3742.957 Hz
55	3753.382 Hz
56	3830.732 Hz
57	3855.823 Hz
58	3916.321 Hz
59	3935.218 Hz
60	3975.383 Hz
61	3993.437 Hz
62	4153.192 Hz
63	4241.321 Hz
64	4243.393 Hz
65	4253.432 Hz
66	4318.222 Hz
67	4375.962 Hz
68	4393.419 Hz
69	4394.134 Hz
70	4417.243 Hz
71	4481.463 Hz
72	4495.138 Hz
73	4549.808 Hz
74	4558.306 Hz
75	4779.451 Hz
76	4838.674 Hz
77	4871.513 Hz
78	4895.296 Hz
79	4962.213 Hz
80	4969.224 Hz
81	4979.321 Hz
82	5027.231 Hz
83	5059.792 Hz
84	5118.094 Hz

85	5176.287 Hz
86	5365.222 Hz
87	5376.392 Hz
88	5426.323 Hz
89	5431.542 Hz
90	5536.242 Hz
91	5739.422 Hz
92	5745.218 Hz
93	5821.975 Hz
94	6037.432 Hz
95	6044.333 Hz
96	6086.256 Hz
97	6208.932 Hz
98	6212.808 Hz
99	6231.031 Hz
100	6280.321 Hz
101	6329.391 Hz
102	6476.896 Hz
103	6477.098 Hz
104	6497.319 Hz
105	6504.983 Hz
106	6651.276 Hz
107	6657.913 Hz
108	6757.901 Hz
109	6758.321 Hz
110	6855.286 Hz
111	6858.121 Hz
112	6898.489 Hz
113	6915.886 Hz
114	7092.219 Hz
115	7120.218 Hz
116	7127.311 Hz
117	7156.489 Hz
118	7208.821 Hz
119	7224.197 Hz
120	7282.169 Hz
121	7285.693 Hz
122	7376.329 Hz
123	7488.742 Hz
124	7577.421 Hz
125	7621.085 Hz
126	7627.207 Hz
127	7650.939 Hz
128	7668.231 Hz

129	7691.212 Hz
130	7842.184 Hz
131	7849.231 Hz
132	7915.423 Hz
133	7932.482 Hz
134	7949.196 Hz
135	7967.311 Hz
136	8021.229 Hz
137	8070.181 Hz
138	8114.032 Hz
139	8149.922 Hz
140	8194.19 Hz
141	8245.801 Hz
142	8328.322 Hz
143	8330.534 Hz
144	8355.987 Hz
145	8408.121 Hz
146	8431.184 Hz
147	8452.119 Hz
148	8548.324 Hz
149	8749.383 Hz
150	8784.424 Hz
151	8894.222 Hz
152	8923.1 Hz
153	8923.361 Hz
154	8935.752 Hz
155	8936.1 Hz
156	9060.323 Hz
157	9072.409 Hz
158	9131.419 Hz
159	9199.232 Hz
160	9245.927 Hz
161	9270.322 Hz
162	9279.193 Hz
163	9393.946 Hz
164	10227.242 Hz
165	10340.509 Hz
166	10363.313 Hz
167	10456.383 Hz
168	10468.231 Hz
169	10470.456 Hz
170	10472.291 Hz
171	10689.339 Hz
172	11525.121 Hz

173	11541.915 Hz
174	11812.419 Hz
175	11840.323 Hz
176	12267.281 Hz
177	12294.283 Hz
178	12629.222 Hz
179	12648.221 Hz
180	13315.335 Hz
181	13735.241 Hz
182	13853.232 Hz
183	13915.231 Hz
184	13990.123 Hz
185	14519.232 Hz
186	14543.128 Hz
187	15651.323 Hz
188	17352.085 Hz
189	17970.122 Hz
190	18524.419 Hz
191	18619.331 Hz
192	18662.112 Hz
193	19385.893 Hz
194	19406.211 Hz
195	